Numerical dispersion and attenuation in the M3 modeling system

Chuck Sword

ABSTRACT

Lattice gases represent a new and interesting approach to the modeling of wave-propagation and fluid-dynamic processes. As pointed out by Muir (1987b), discrete lattice gases can be generalized as ensembles, and calculations can be carried out on probability values rather than on the individual particles. Furthermore, the probability values can be linearized, resulting in the M3 modeling system. A method has been developed that allows the calculation of the dispersion (phase velocity versus spatial frequency), attenuation (decrease in amplitude with respect to time), and anisotropy of acoustic waves in the M3 system. These numerical results can, in turn, be applied to the original lattice-gas method. They confirm theoretical results (d'Humieres et al., 1986) regarding the isotropy of certain lattices.

INTRODUCTION

Lattice gases in general, and the M3 method (Muir, 1987b) in particular, represent an interesting addition to the repertoire of acoustic modeling methods. It is useful to examine the numerical dispersion, attenuation, and anisotropy of the M3 method; by analyzing such properties we are better able to evaluate the usefulness of the M3 method in comparison with other, more traditional modeling methods. We are also able to check the results of some theoretical studies of lattice gases.

NOTATION

The lattice-gas model consists of a grid, with particles traveling along the lines of the grid and interacting at the intersections of these lines. In the M2 and M3 models, the discrete particles are replaced by probability values. A system of notation must

be developed in order to keep track of these particles or probabilities as they travel around the grid.

The M2 method

Let u represent the probability that a given particle exists. The M2 method (Muir, 1987b) provides a way of determining the rules that govern these probabilities, without requiring that individual particles be considered. Since u is a probability, it can take a value in the range $0 \leq u \leq 1$.

Suppose a particle (or rather, a probability value u) has just left an intersection (also called a vertex), and is headed along a grid line towards the next intersection. It leaves the intersection at time t, so at that moment it carries the value u^t. It approaches that next intersection at time $t + 1 - \epsilon$ (ϵ is a number much smaller than 1), at which time it carries the value $u^{t+1-\epsilon}$. In accordance with the lattice-gas model, u does not change until it actually reaches that next intersection, so $u^{t+1-\epsilon} = u^t$. Finally it reaches the intersection, collides with other particles, and heads away from the intersection. As it heads away, the time is now $t + 1$, and the particle has a probability u^{t+1}. In general, u^{t+1} does not equal u^t; the rules connecting u^t and u^{t+1} will be given below. Note the assumption, made without loss of generality, that Δt, the travel time between intersections, equals 1. This travel time is the same for all particles at all locations on the grid.

Each value u, besides carrying a superscript designating time, carries subscripts designating direction of travel and location. Figure 1 shows how this notation works. Each vertex (intersection) on the grid is designated by a letter of the alphabet. In the case of a hexagonal grid, it is convenient to designate the central point by the letter o, and its nearest neighbors by the letters a through f. Each direction of travel is designated by a number. Thus, in Figure 1 the probability value of the particle leaving vertex o at time t, and traveling towards vertex a, is u^t_{o1}. As this particle approaches vertex a, it has the probability $u^{t+1-\epsilon}_{a1}$ (note how o has been replaced by a in the subscript). After it has collided with other particles, and passed through vertex a, it has the value u^{t+1}_{a1}. As before,

$$u^t_{o1} = u^{t+1-\epsilon}_{a1} \neq u^{t+1}_{a1}. \tag{1}$$

In general, for the grid shown in Figure 1,

$$\begin{pmatrix} u^t_{o1} & u^t_{o2} & u^t_{o3} & u^t_{o4} & u^t_{o5} & u^t_{o6} \end{pmatrix}^{\mathrm{T}} = \tag{2}$$
$$\begin{pmatrix} u^{t+1-\epsilon}_{a1} & u^{t+1-\epsilon}_{b2} & u^{t+1-\epsilon}_{c3} & u^{t+1-\epsilon}_{d4} & u^{t+1-\epsilon}_{e5} & u^{t+1-\epsilon}_{f6} \end{pmatrix}^{\mathrm{T}}.$$

Likewise,

$$\begin{pmatrix} u^t_{d1} & u^t_{e2} & u^t_{f3} & u^t_{a4} & u^t_{b5} & u^t_{c6} \end{pmatrix}^{\mathrm{T}} = \tag{3}$$
$$\begin{pmatrix} u^{t+1-\epsilon}_{o1} & u^{t+1-\epsilon}_{o2} & u^{t+1-\epsilon}_{o3} & u^{t+1-\epsilon}_{o4} & u^{t+1-\epsilon}_{o5} & u^{t+1-\epsilon}_{o6} \end{pmatrix}^{\mathrm{T}}.$$

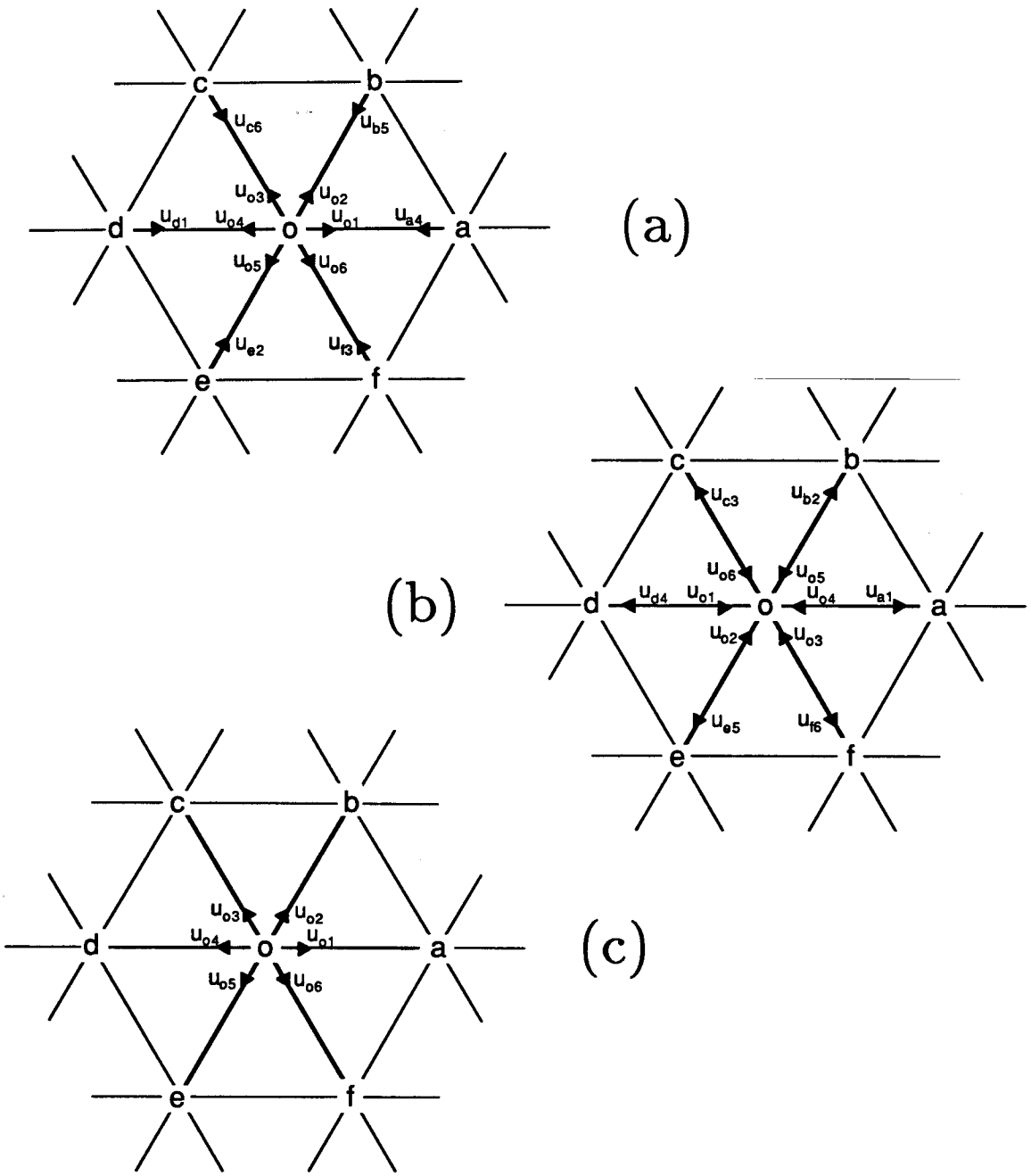

FIG. 1. Notation. The three panels in this figure show particle positions as a function of time. Panels (a), (b), and (c) represent times t , $t+1-\epsilon$, and $t+1$, respectively. Note how each node of the hexagonal grid is given a letter, and each direction of travel is given a number. Any particle (or probability value) on the grid can be specified by grid location and travel direction. Normally there would be superscripts on the u's to denote time. These have been omitted for the sake of clarity.

Linearization: the M3 method

Suppose that u equals $1/2 + \alpha u'$, where α is small. This value of u can be used to linearize the M2 method; the result is the M3 method. The M3 method thus shows how to propagate values of the perturbation u'. This paper will, for the most part, discuss aspects of the M3 method. Note that u' is a probability perturbation rather than an actual probability, so it can take both positive and negative values. For most of this paper, the prime will be dropped from u'.

CALCULATING THE M3 COLLISION MATRIX

The collision matrix is the matrix that tells how the values of $u^{t-\epsilon}$ are transformed, via collisions at the vertices, to values of u^t. This matrix can be determined only for the M3 method; the collision rules for the M2 method are non-linear.

Conservation laws

Let us begin with the M2 model, where each value of u represents the probability that a given particle exists. The particles have mass and momentum; these quantities must be conserved (Muir, 1987b). Between collisions, from time t to time $t+1-\epsilon$, these quantities are automatically conserved, since the particles (probability values) are traveling along straight lines between vertices. Care must be taken, however, to conserve these quantities before and after collision at each vertex.

Specifically, there are three conserved quantities: mass m, east-west momentum p_x, and north-south momentum p_y. Let $\mathbf{u}_o^t$ be defined as follows:

$$\mathbf{u}_o^t \equiv \begin{pmatrix} u_{o1}^t & u_{o2}^t & u_{o3}^t & u_{o4}^t & u_{o5}^t & u_{o6}^t \end{pmatrix}^{\mathrm{T}}. \tag{4}$$

Let $\underset{\sim}{\mathbf{C}}$ be the matrix that determines the values of the conserved quantities, given the $\mathbf{u}$ vector at a vertex (in this case, vertex o):

$$\underset{\sim}{\mathbf{C}}\mathbf{u}_o^t = \begin{pmatrix} m \\ p_x \\ p_y \end{pmatrix}. \tag{5}$$

Let vertex a be located at (x_a, y_a), vertex b be located at (x_b, y_b), and so forth. Let vertex o be located at $(x_o, y_o) = (0, 0)$. Furthermore, let all the vertices be equidistant. If the geometry is hexagonal, as shown in Figure 1, and the particles are examined just *after* collision, then at vertex o,

$$\underset{\sim}{\mathbf{C}} = \begin{pmatrix} 1 & 1 & 1 & 1 & 1 & 1 \\ x_a & x_b & x_c & x_d & x_e & x_f \\ y_a & y_b & y_c & y_d & y_e & y_f \end{pmatrix}. \tag{6}$$

Each particle is assumed to have mass 1. The momentum terms are off by a factor of $1/\Delta t$, where Δt is the time step.

The conservation of mass and momentum before and after collision can now be expressed by the formula

$$\underset{\sim}{C}\mathbf{u}_o^t = \underset{\sim}{C}\mathbf{u}_o^{t-\epsilon}. \tag{7}$$

This formula is a linear constraint on the values of $\mathbf{u}_o^t$, given $\mathbf{u}_o^{t-\epsilon}$. This constraint holds for the M2 modeling system, and it holds for the M3 linearized model as well.

Note that if the distances between vertices are all the same, then conservation of mass implies conservation of energy. Recall that kinetic energy $KE = mv^2/2$. Particle speed v is constant if the distances between vertices are all the same; as a result, kinetic energy is proportional to mass. There are no potential fields in this modeling scheme, so potential energy plays no role; it is necessary only to consider kinetic energy.

Maximization condition for M2

M2 is defined by Muir (1987b) in terms of a maximum-entropy principle: the entropy of the probability vector $\mathbf{u}_o^t$ should be maximized after each collision. In other words, the amount of information about the history of the particles should be minimized. This approach therefore differs from approaches that seek to make the collision process reversible. Entropy is given by the formula:

$$S_o^t = -\sum_{i=1}^{N} \left[u_{oi}^t \log_2 u_{oi}^t + (1 - u_{oi}^t) \log_2 (1 - u_{oi}^t) \right]. \tag{8}$$

Here S_o^t is the entropy at vertex o at time t, and N is the number of lines converging at this vertex. Thus, the collision rules in the M2 system are determined by finding the value of $\mathbf{u}_o^t$ that maximizes S in equation (8), while fulfilling the linear constraint in equation (7). There is no known closed-form solution for this constrained non-linear maximization problem.

Maximization condition for M3

Figure 2 shows a graph of entropy versus the value of u, based on a single term in the sum in equation (8). Note that the entropy has a maximum when $u = 1/2$. Suppose, then, that $u = 1/2 + \alpha u'$, where α is small. To first order, equation (8) becomes:

$$S_o^t \approx \sum_{i=0}^{N} \left(1 - \frac{2}{\ln 2} \alpha^2 {u'_{oi}}^2 \right) = N - \frac{2\alpha^2}{\ln 2} \sum_{i=1}^{N} {u'_{oi}}^2. \tag{9}$$

The constants can be ignored, so maximizing entropy is now equivalent to minimizing $\sum_{i=1}^{N} u_{oi}^2$, where the prime has been dropped from u'. In other words, the entropy is maximized when $|\mathbf{u}_o^t|^2$ is minimized (Muir, 1987b).

Collision rules in the M3 linearized system are thus determined by a simple linear minimization condition, and a set of linear constraints.

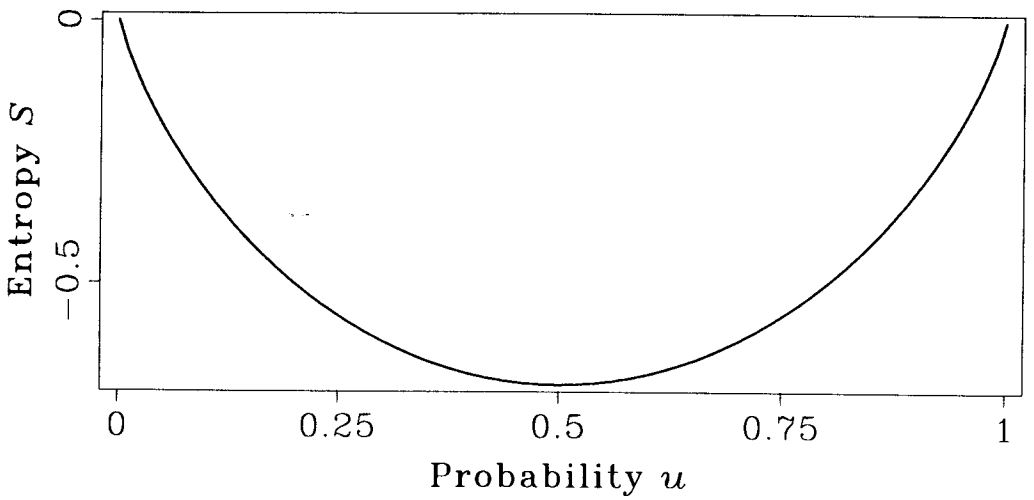

FIG. 2. Entropy versus probability. Shown is a graph of entropy S versus probability u, based on a single term of the sum in equation (8). Note the maximum at $u = 1/2$.

Four-dimensional grids and weighting matrices

So far only a simple hexagonal grid has been discussed. It is necessary to examine more complicated grids if one is interested in modeling three-dimensional systems. It has been shown (d'Humieres et al., 1986) that isotropic modeling results can be obtained only for certain grids. One of these grids is the two-dimensional hexagonal grid; another is a four-dimensional rectangular grid with lines connecting each point to its 24 next-nearest neighbors. This four-dimensional grid can be projected onto three dimensions for isotropic three-dimensional modeling, or even onto two dimensions (Muir, 1987a). Figure 3a shows the two-dimensional projection of this four-dimensional grid. The numbers in this figure show the number of lines in 4-space that have been superimposed onto each line in 2-space. In all, 24 lines have been projected onto 9 lines. Only 8 of these 9 lines are visible; the 9th is an out-of-plane line connecting the central vertex to itself.

The concept of projecting four dimensions onto two is rather unconventional; it is helpful to describe explicitly the constraint matrix and the minimization condition for the M3 version of this grid. Figure 3b shows how the lines are numbered in this example; note that the out-of-plane line is number 9. Now

$$\mathbf{u}_o^t = \begin{pmatrix} u_{o1}^t & u_{o2}^t & u_{o3}^t & u_{o4}^t & u_{o5}^t & u_{o6}^t & u_{o7}^t & u_{o8}^t & u_{o9}^t \end{pmatrix}^{\mathrm{T}}, \tag{10}$$

and the constraint matrix is written as:

$$\underset{\sim}{\mathbf{C}} = \begin{pmatrix} 4 & 1 & 4 & 1 & 4 & 1 & 4 & 1 & 4 \\ 4x_a & x_b & 4x_c & x_d & 4x_e & x_f & 4x_g & x_h & 4x_o \\ 4y_a & y_b & 4y_c & y_d & 4y_e & y_f & 4y_g & y_h & 4y_o \end{pmatrix}. \tag{11}$$

Recall that $x_o = y_o = 0$. Notice the factors of four that appear in equation (11). These arise because of the multiple paths that are shown in Figure 3a. Each particle

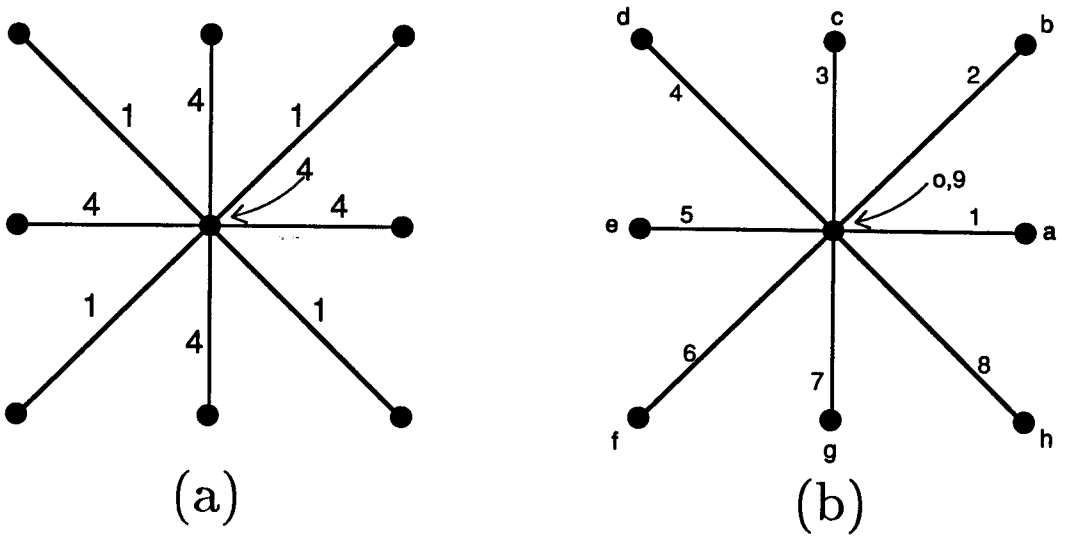

FIG. 3. Rectangular grid. This is the two-dimensional projection of a four-dimensional grid. Panel (a) shows the number of lines in 4-space that project onto each line in 2-space. Panel (b) shows the notational system for this grid. Numbers represent directions, and letters represent grid points.

on the projected two-dimensional grid represents either one or four particles on the original four-dimensional grid.

It was previously noted that for energy to be proportional to mass, the grid lines must all be of equal length, so that particle velocity is constant. This condition is fulfilled, despite appearances, by the grid in Figure 3a. Although the two-dimensional lines differ in length, they are all the same length in 4-space. Even the path that connects the vertex to itself is the same length as the other paths; it seems to be of zero length only because it is entirely in the out-of-plane direction. Particles traveling on this out-of-plane path have the same kinetic energy as particles on any of the other paths. Kinetic energy, therefore, remains proportional to particle mass.

The matrix in equation (11) can be simplified by applying a weighting matrix $\underset{\sim}{\mathbf{W}}$, where matrix elements $W_{ij} = w_i \delta_{ij}$. Note that by this definition, $\underset{\sim}{\mathbf{W}}$ is diagonal. The weighting elements w_i are given by:

$$\begin{pmatrix} w_1 & w_2 & w_3 & w_4 & w_5 & w_6 & w_7 & w_8 & w_9 \end{pmatrix}^{\mathrm{T}} = \begin{pmatrix} 4 & 1 & 4 & 1 & 4 & 1 & 4 & 1 & 4 \end{pmatrix}^{\mathrm{T}}. \tag{12}$$

Once $\underset{\sim}{\mathbf{W}}$ is defined, the constraint matrix can be written:

$$\underset{\sim}{\mathbf{C}} = \begin{pmatrix} 1 & 1 & 1 & 1 & 1 & 1 & 1 & 1 & 1 \\ x_a & x_b & x_c & x_d & x_e & x_f & x_g & x_h & x_o \\ y_a & y_b & y_c & y_d & y_e & y_f & y_g & y_h & y_o \end{pmatrix}, \tag{13}$$

where

$$\underset{\sim}{\mathbf{C}}\underset{\sim}{\mathbf{W}}\mathbf{u}_o^t = \begin{pmatrix} m \\ p_x \\ p_y \end{pmatrix}. \tag{14}$$

As with equation (5), the momenta are off by a factor of $1/\Delta t$. The linear constraint equation now becomes

$$\underset{\sim}{\mathbf{C}}\underset{\sim}{\mathbf{W}}\mathbf{u}_o^t = \underset{\sim}{\mathbf{C}}\underset{\sim}{\mathbf{W}}\mathbf{u}_o^{t-\epsilon}. \tag{15}$$

Following the principle that each particle in 2-space represents one or more particles in 4-space, the M3 maximum-entropy condition is equivalent to minimizing $\sum_{i=1}^{9}(u_{oi}^t w_i)^2$. In other words, it is equivalent to minimizing $|\underset{\sim}{\mathbf{W}}\mathbf{u}_o^t|^2$.

Solving the minimization problem

Once the weighting matrix $\underset{\sim}{\mathbf{W}}$ has been introduced, it is possible to find a general formula for the shuffling matrix. This matrix is designated $\underset{\sim}{\mathbf{A}}$, and its function, shuffling, can be represented as:

$$\mathbf{u}_o^t = \underset{\sim}{\mathbf{A}}u_o^{t-\epsilon}. \tag{16}$$

The matrix $\underset{\sim}{\mathbf{A}}$ must fulfill the constraints in equation (15) and the minimization condition on $|\underset{\sim}{\mathbf{W}}\mathbf{u}_o^t|^2$. It can be shown, then, that

$$\underset{\sim}{\mathbf{A}} = \underset{\sim}{\mathbf{W}}^{-1}\underset{\sim}{\mathbf{W}}^{\mathrm{T}}\underset{\sim}{\mathbf{C}}^{\mathrm{T}}(\underset{\sim}{\mathbf{C}}\underset{\sim}{\mathbf{W}}^{\mathrm{T}}\underset{\sim}{\mathbf{C}}^{\mathrm{T}})^{-1}\underset{\sim}{\mathbf{C}}\underset{\sim}{\mathbf{W}}. \tag{17}$$

Note that $\underset{\sim}{\mathbf{C}}$ is the *unweighted* constraint matrix, similar to that in equation (13) or (6).

Equation (17) can be rewritten in the language of Moore-Penrose inverses (Muir, 1987a). Recall that $\underset{\sim}{\mathbf{W}}$ is defined to be diagonal. Assume that $\underset{\sim}{\mathbf{W}}$ is also non-singular (that is, that there are no zero weights). If the transformation matrix is written as $\underset{\sim}{\mathbf{T}}$, then

$$\underset{\sim}{\mathbf{T}} = \underset{\sim}{\mathbf{C}}\underset{\sim}{\mathbf{W}}, \tag{18}$$

and the Moore-Penrose inverse is written:

$$\underset{\sim}{\mathbf{T}}^{\dagger} = \underset{\sim}{\mathbf{C}}^{\mathrm{T}}(\underset{\sim}{\mathbf{C}}\underset{\sim}{\mathbf{W}}\underset{\sim}{\mathbf{C}}^{\mathrm{T}})^{-1}. \tag{19}$$

By substitution from equation (17) it can be shown that $\underset{\sim}{\mathbf{A}}\underset{\sim}{\mathbf{A}} = \underset{\sim}{\mathbf{A}}$, meaning that $\underset{\sim}{\mathbf{A}}$ is idempotent. For the hexagonal grid,

$$\underset{\sim}{\mathbf{A}} = \begin{pmatrix} 1/2 & 1/3 & 0 & -1/6 & 0 & 1/3 \\ 1/3 & 1/2 & 1/3 & 0 & -1/6 & 0 \\ 0 & 1/3 & 1/2 & 1/3 & 0 & -1/6 \\ -1/6 & 0 & 1/3 & 1/2 & 1/3 & 0 \\ 0 & -1/6 & 0 & 1/3 & 1/2 & 1/3 \\ 1/3 & 0 & -1/6 & 0 & 1/3 & 1/2 \end{pmatrix}. \tag{20}$$

The first line of this matrix was previously given by Muir (1987b).

DISPERSION, ATTENUATION, AND ANISOTROPY: THEORY

Every numerical modeling scheme suffers from a certain amount of anisotropy (phase velocity varying as a function of propagation direction) and frequency dispersion (phase velocity varying as a function of spatial frequency). Some schemes also suffer from attenuation (damping in time as a function of spatial frequency). Quantitative estimates of these effects are useful, because they allow comparison of different modeling methods.

Shuffling and advection matrices

Recall equation (3), which shows how $\mathbf{u}_o^{t+1-\epsilon}$ is made up of values of u from the nearest neighbors at the previous time step. Equation (3) might be called an advection equation (Muir, 1987b), since it describes how values of u propagate from vertex to vertex. Given the advection equation, and the shuffling matrix $\underset{\sim}{\mathbf{A}}$ from equation (17), it is possible to obtain estimates of dispersion, anisotropy, and attenuation.

Conversion to the Fourier domain

To estimate dispersion (as well as the other quantities), it is necessary to transform u from the time and space domains to the domains of temporal and spatial frequency. Suppose that u_{lm}^t is the probability value traveling in direction m at time t and at point l. Furthermore, suppose that point l is located at $\mathbf{x}_l = (x_l, y_l)$. Now let $u(x, y, t)$ be replaced by a spatially monochromatic wave of spatial frequency $\mathbf{k} = (k_x, k_y)$ and temporal frequency ω. Then

$$u_{lm}^t = c_m e^{i(\omega t - \mathbf{k}\cdot\mathbf{x})}, \tag{21}$$

where c_m is some complex constant.

Equations (3), (16), and (21) can be combined to show:

$$\underset{\sim}{\mathbf{A}} \begin{pmatrix} c_1 e^{i(\omega t-\mathbf{k}\cdot\mathbf{x}_d)} & c_2 e^{i(\omega t-\mathbf{k}\cdot\mathbf{x}_e)} & c_3 e^{i(\omega t-\mathbf{k}\cdot\mathbf{x}_f)} & c_4 e^{i(\omega t-\mathbf{k}\cdot\mathbf{x}_a)} & c_5 e^{i(\omega t-\mathbf{k}\cdot\mathbf{x}_b)} & c_6 e^{i(\omega t-\mathbf{k}\cdot\mathbf{x}_c)} \end{pmatrix}^{\mathrm{T}}$$
$$= \begin{pmatrix} c_1 e^{i\omega(t+1)} & c_2 e^{i\omega(t+1)} & c_3 e^{i\omega(t+1)} & c_4 e^{i\omega(t+1)} & c_5 e^{i\omega(t+1)} & c_6 e^{i\omega(t+1)} \end{pmatrix}^{\mathrm{T}}. \tag{22}$$

Recall that $\mathbf{x}_o = (0, 0)$.

Solving the eigenvalue problem

Let

$$\mathbf{c} \equiv \begin{pmatrix} c_1 & c_2 & c_3 & c_4 & c_5 & c_6 \end{pmatrix}^{\mathrm{T}}. \tag{23}$$

Equation (22) can be re-written as

$$\underset{\sim}{\mathbf{R}}\mathbf{c} = e^{i\omega}\mathbf{c}, \tag{24}$$

where

$$\underset{\approx}{\mathbf{R}} \equiv \left(\underset{\approx}{\mathbf{A}}\right) \begin{pmatrix} e^{-i\mathbf{k}\cdot\mathbf{x}_d} & & & & & \\ & e^{-i\mathbf{k}\cdot\mathbf{x}_e} & & & & \\ & & e^{-i\mathbf{k}\cdot\mathbf{x}_f} & & 0 & \\ & & & e^{-i\mathbf{k}\cdot\mathbf{x}_a} & & \\ & 0 & & & e^{-i\mathbf{k}\cdot\mathbf{x}_b} & \\ & & & & & e^{-i\mathbf{k}\cdot\mathbf{x}_c} \end{pmatrix}. \tag{25}$$

Note that $\mathbf{k}$ is given, so equation (24) is an eigenvalue equation for the unknowns ω and $\mathbf{c}$. Thus, solving equation (24) will give ω as a function of $\mathbf{k}$. If ω is unchanging as $|\mathbf{k}|$ varies, then the modeling method has no dispersion. If ω is unchanging as $\mathbf{k}$ varies while $|\mathbf{k}|$ is constant, then the modeling method is isotropic. If ω is real (not complex), then the modeling method has no attenuation.

NUMERICAL RESULTS

The complex-value eigenvalue problem in equation (24) can be solved numerically. If λ is defined such that

$$\lambda = e^{i\omega}, \tag{26}$$

then $Re\ \omega = \tan^{-1}(Re\,\lambda / Im\,\lambda)$. Phase velocity v obeys the formula $v = (Re\ \omega)/|\mathbf{k}|$. If $|\lambda| < 1$, then the amplitude of the wave decays over time.

The dispersion, anisotropy, and attenuation of three different M3 grids will be examined: hexagonal, rectangular, and projected four-dimensional. A conventional explicit finite-differencing scheme will be used as a control.

In order for comparisons of the gridding schemes to be valid, the grids must conform to a uniform standard. Standardization is obtained by regularizing grid density: the grids are scaled so as to ensure that they all have the same number of grid points (vertices) per unit area. The plots that follow can therefore be directly compared with one another.

The hexagonal grid

The first grid is the hexagonal one shown in Figure 1. The attenuation of this grid is shown in Figure 4. The most obvious feature on this figure, a region of irregular contours, is a numerical artifact. A double-precision Eispack subroutine was used to find eigenvalues and eigenvectors; for certain values of $\mathbf{k}$ near the Nyquist frequency, this subroutine had difficulty. Note the aliasing effects in regions with frequencies higher than the spatial Nyquist.

The significance of Figure 4 is that it shows that for a hexagonal grid, attenuation is an important factor except at the lowest frequencies. Even at one third of the Nyquist frequency, the amplitude decays by 10% at each time step. At higher frequencies, the anisotropy increases, forming a pattern that is hexagonally symmetric.

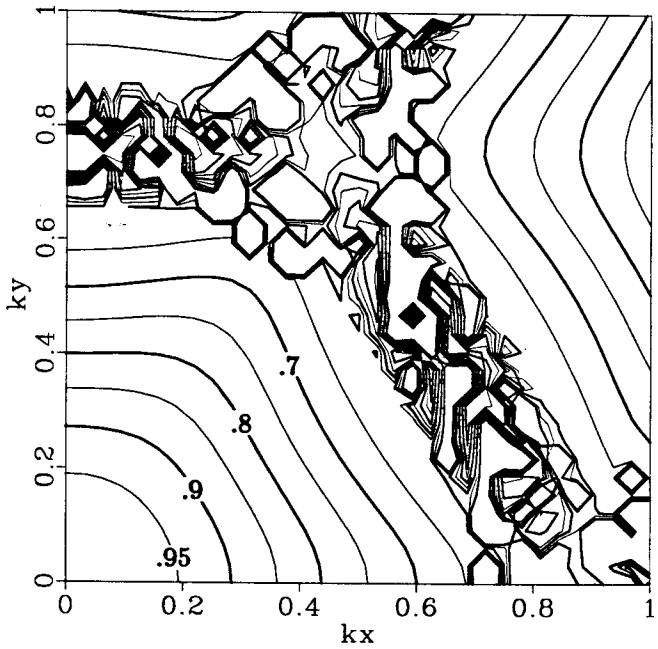

FIG. 4. Attenuation on a hexagonal grid. Attenuation is shown as a function of k_x and k_y. The contour lines show the relative wave amplitudes after a single time step. Artifacts are visible near the spatial Nyquist frequencies. Because of aliasing, the attenuation pattern appears to repeat itself beyond the Nyquist.

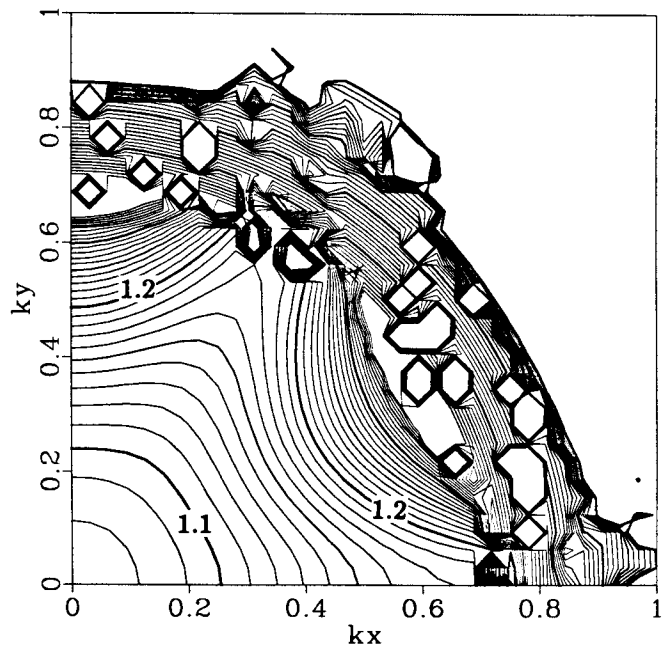

FIG. 5. Phase velocity on a hexagonal grid. Phase velocity is shown as a function of k_x and k_y. The contour lines show the distance covered by a monochromatic wave in a single time step. The velocity is isotropic at low frequencies, and hexagonally anisotropic at higher frequencies.

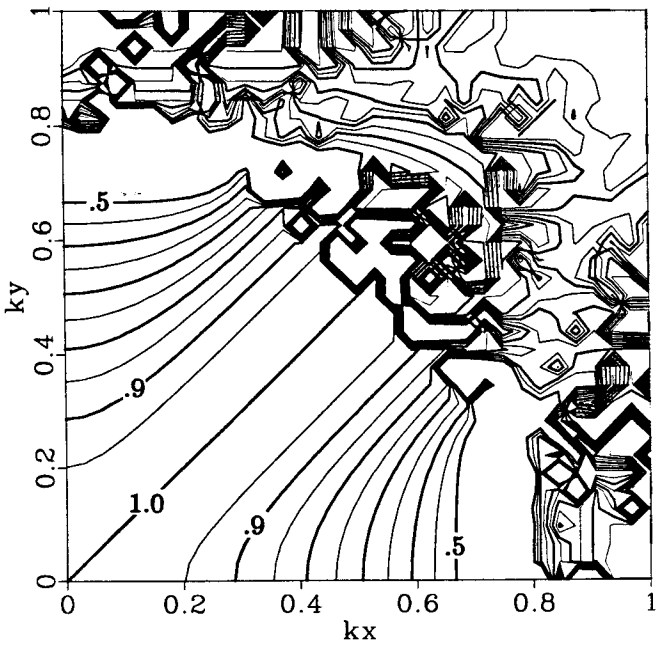

FIG. 6. Attenuation on a rectangular grid. Attenuation is shown as a function of k_x and k_y. The contour lines show the relative wave amplitude after a single time step. Waves traveling at 45 degrees to the x and y axes are not attenuated at all.

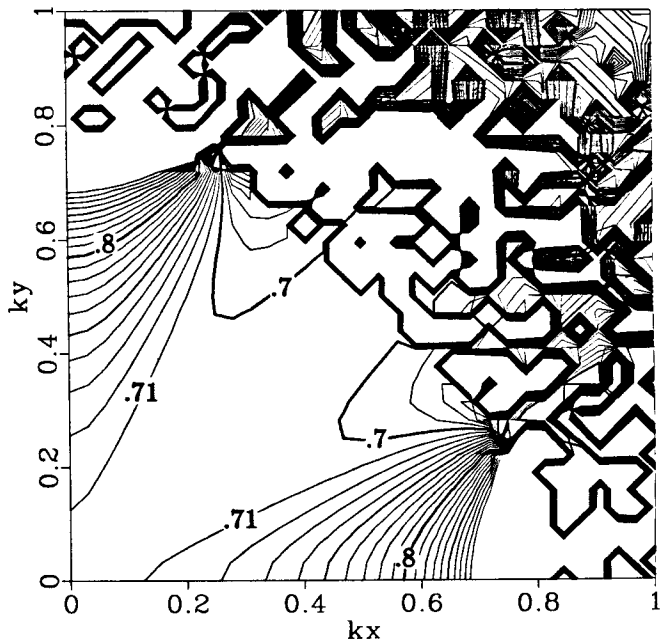

FIG. 7. Phase velocity on a rectangular grid. Phase velocity is shown as a function of k_x and k_y. The contour lines show the distance covered by a monochromatic wave in a single time step. Waves traveling at 45 degrees to the x and y axes do not undergo frequency dispersion.

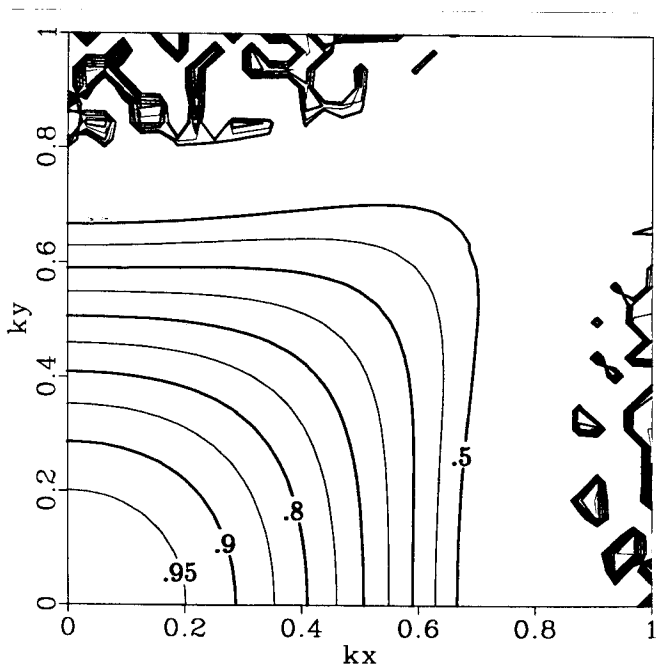

FIG. 8. Attenuation on the projected four-dimensional grid. Attenuation is shown as a function of k_x and k_y. The contour lines show the relative wave amplitude after a single time step.

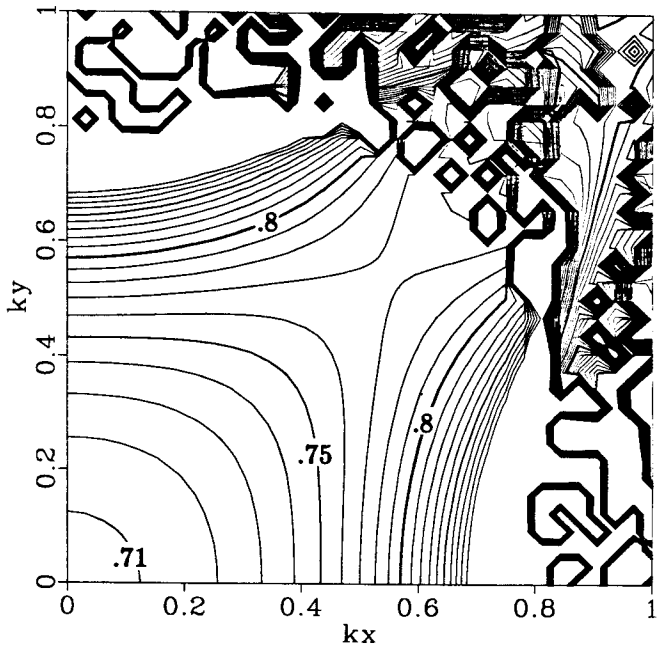

FIG. 9. Phase velocity on the projected four-dimensional grid. Phase velocity is shown as a function of k_x and k_y. The contour lines show the distance covered by a monochromatic wave in a single time step.

Figure 5 shows the phase velocity for a hexagonal grid. At the lowest spatial frequencies, dispersion and anisotropy are not significant problems, but at higher frequencies they are more so.

The rectangular grid

Many early lattice-gas schemes used a simple rectangular grid (Hardy et al., 1976). The attenuation of this grid is shown in Figure 6. In this plot, the spatial Nyquist frequencies are at $k_x = 1.0$ and $k_y = 1.0$. Along a diagonal line, there is no attenuation at all, but the attenuation becomes greater as distance from this line increases. Figure 7 shows the behavior of the phase velocity. Even at low frequencies there is anisotropy. Based on Figures 6 and 7, one would expect a point source to produce a wave that travels faster vertically and horizontally than diagonally, but that dies out in all but the diagonal direction. Numerical experiments confirm this prediction.

The projected four-dimensional grid

A projected four-dimensional grid was shown in Figure 3. Figure 8 shows the attenuation characteristics of this grid. As with the hexagonal grid, attenuation becomes significant (greater than 10%) when $|\mathbf{k}|$ is greater than about .25·Nyquist. Figure 9 shows the phase velocity. It is isotropic and not significantly dispersive at lower spatial frequencies.

The propagation velocity for this grid can be varied by varying the weighting of the center point (the out-of-plane path). This corresponds to varying w_9 in equation (12). The phase velocity at low frequencies remains isotropic for such variations.

Finite-differencing grids

For comparison, the dispersion relation of an explicit finite-differencing scheme is examined. A simple finite differencing scheme, second-order in time and fourth-order in space, can be written as:

$$u_{i,j}^{t+1} - 2u_{i,j}^{t} + u_{i,j}^{t-1} = -\frac{1}{v^2}\left(-\frac{1}{12}u_{i-2,j}^{t} + \frac{4}{3}u_{i-1,j}^{t} + \frac{4}{3}u_{i+1,j}^{t} - \frac{1}{12}u_{i+2,j}^{t} - \right.$$
$$\left. -\frac{1}{12}u_{i,j-2}^{t} + \frac{4}{3}u_{i,j-1}^{t} + \frac{4}{3}u_{i,j+1}^{t} - \frac{1}{12}u_{i,j+2}^{t} - \frac{30}{6}u_{i,j}^{t}\right). \qquad (27)$$

In this equation, $u_{i,j}^{t}$ refers to the pressure at time t and at grid location i, j. The velocity v controls the low-frequency phase velocity. Let $\Delta t = .5$ and $\Delta x = \Delta y = 1$; Figure 10 shows the phase velocity when $v = \sqrt{2}/2$. Note that Δt is half the timestep used in M3 modeling. The finite-differencing scheme is unstable for $v = \sqrt{2}/2$ when $\Delta t = 1$. No graph is given for attenuation, since such explicit finite-differencing schemes have no attenuation within the stability limits.

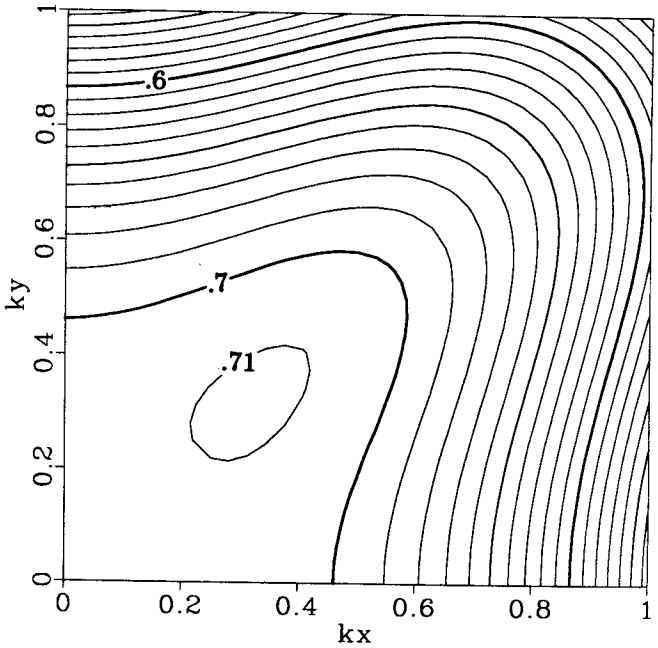

FIG. 10. Phase velocity for a fourth-order finite-differencing scheme. Phase velocity is shown as a function of k_x and k_y. The contour lines show the distance covered by a monochromatic wave in a single time step. Despite the apparent anisotropy, velocity is nearly constant at low frequencies.

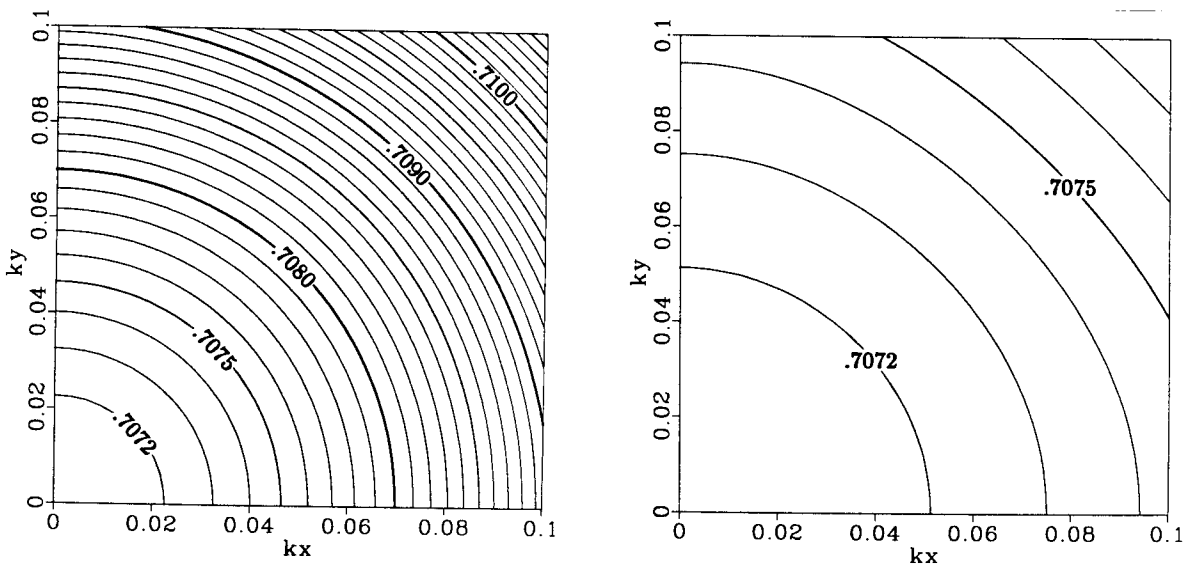

FIG. 11. Comparison of phase velocity at low frequencies. The contour plots in Figures 9 and 10 are magnified for comparison. Phase velocities are isotropic, and the dispersion is not large.

Figure 11 shows magnified versions of Figure 9 (phase velocity for the projected four-dimensional M3 scheme) and Figure 10. It is apparent that at low spatial frequencies, both the M3 and the finite-differencing scheme are isotropic. The finite-differencing method has less dispersion than the M3 method, and it has no attenuation.

DISCUSSION

The M3 model behaves like a physical acoustic medium in many ways, but it exhibits some interesting differences as well. For instance, mass density in M3 seems to correspond to pressure in physical media. On the other hand, waves dissipate in the M3 model but are conserved in non-viscous physical media.

Apples and oranges

Is it valid to compare finite-differencing and M3 schemes? Are they modeling similar quantities? The finite-difference method is modeling pressure. The M3 scheme is measuring the probability that there is a particle in a certain location, moving with a certain speed. I would argue that these two quantities are similar. Pressure, after all, is related to the number of particles in one spot, and the number of particles is what is given (in a statistical sense) by M3. It appears, then, that these two seemingly unrelated modeling methods can be compared, with pressure in a conventional gas corresponding to mass density in a lattice gas.

Where does the energy go?

The energy of particles is conserved at every collision; as noted above, conservation of energy is a consequence of conservation of mass when the grid is regular. It seems paradoxical, then, that a spatially monochromatic wavefield could attenuate and gradually fade away. Where does the energy go? The surprising answer is that waves in a lattice gas, unlike waves in a conventional gas, carry information but not energy. Thus, there is no energy to be lost as the waves fade away.

In a lattice gas, a monochromatic wave has zero energy overall. Recall that kinetic energy is directly proportional to mass, since velocity does not vary. Some regions of the wave have positive values of u (mass), and therefore positive kinetic energy, Other regions have negative values of u, with consequent negative values of kinetic energy. (Of course, M3 is a linearized perturbation of M2; positive and negative values of mass or energy in M3 should be understood to mean positive and negative perturbations on a constant background.) The spatially averaged energy of a wave is therefore zero, independent of its amplitude.

Waves in a lattice gas therefore do not carry energy. Waves in a conventional gas, however, do. This difference is a consequence of the fact that particles in a lattice gas travel at a constant speed, independent of density changes in the gas: if a lattice gas is compressed or rarefied, its energy density (energy per unit area)

varies, but its temperature (average speed per particle) does not. In a conventional gas, on the other hand, temperature, and thus particle velocity, increases with compression. Denser regions in a conventional acoustic wave have higher energy, as a result of both an increased particle density and an increased energy (temperature) per particle. This increased energy is *not* canceled out by the lower energy in the rarefied regions of the wavefield. Thus, the overall energy is non-zero for a wave in a conventional gas.

Although the energy of a monochromatic wave in a lattice gas is independent of amplitude, its entropy is not. Recall that the M2 (and M3) shuffling procedure seeks to maximize entropy. As a result, entropy (disorder) remains constant or increases with each time step. Ordered states, such as waves, slowly decay into disorder. This disorder is not visible: M2 and M3 represent averages over an ensemble, so the disorder averages out.

CONCLUSIONS

A comparison among the various M3 grids shows that the best M3 scheme is based on a four-dimensional grid projected onto a two-dimensional plane. This grid exhibits better isotropy than the hexagonal grid, and is computationally simpler to use. The main disadvantages of the M3 scheme, compared to a conventional fourth-order finite-differencing method, are that the wavefield dies out over time, and that low-frequency waves are more dispersive. Further studies are needed to decide whether the attenuation presents a serious problem, and to determine whether the M3 approach has advantages (such as better behavior at the model boundaries) that outweigh its disadvantages.

It may be possible to linearize other lattice-gas schemes, and subject them to dispersion analysis. Such an analysis would give an idea of how well lattice gases model acoustic waves. A problem with lattice gases is that they are always at a constant temperature; as a result of this constant temperature, waves in a lattice gas carry no energy. It may be interesting to consider variable-temperature lattice-gas models.

ACKNOWLEDGMENTS

This paper would not have been possible without the constant guidance and the useful insights of Francis Muir. Besides giving me the benefit of his experience with lattice gases, he was kind enough to allow me to discuss techniques, such as the projected four-dimensional grid, that he has not yet fully published. His wisdom and his generosity helped me a great deal. I also benefited from discussions with Fabio Rocca and Dan Rothman; John Etgen provided me with the fourth-order finite-differencing star.

REFERENCES

Hardy, J., de Pazzis, O., and Pomeau, Y., 1976, Molecular dynamics of a classical lattice gas: Phys. Rev. A, **13**, 1949.

d'Humieres, D., Lallemand, P., and Frisch, U., 1986, Lattice gas models for 3D hydrodynamics: Europhys. Lett., **2** (4), 291–297

Muir, F., 1987a, M3 to M4: from Huygens' to conservation variables: SEP–56, this report.

Muir, F., 1987b, Three experimental modeling systems: SEP–51, 119–128.